Tomography of pions and protons via transverse momentum dependent distributions

P. C. Barry,[1] L. Gamberg,[2] W. Melnitchouk,[1,3] E. Moffat,[2,4] D. Pitonyak,[5] A. Prokudin,[1,2] and N. Sato[1]
(**Jefferson Lab Angular Momentum (JAM) Collaboration**)
[1] *Jefferson Lab, Newport News, Virginia 23606, USA*
[2] *Division of Science, Penn State Berks, Reading, Pennslyvania, 19610, USA*
[3] *CSSM and CDMPP, Department of Physics, University of Adelaide, Adelaide 5000, Australia*
[4] *Physics Division, Argonne National Laboratory, Lemont, Illinois 60439, USA*
[5] *Department of Physics, Lebanon Valley College, Annville, Pennsylvania 17003, USA*
(Dated: January 30, 2023)

We perform the first simultaneous extraction of parton collinear and transverse degrees of freedom from low-energy fixed-target Drell-Yan data in order to compare the transverse momentum dependent (TMD) parton distribution functions (PDFs) of the pion and proton. We demonstrate that the transverse separation of the quark field encoded in TMDs of the pion is more than 5σ smaller than that of the proton. Additionally, we find the transverse separation of the quark field decreases as the longitudinal momentum fraction decreases. In studying the nuclear modification of TMDs, we observe that it is similar to that found in collinear distributions. We comment on possible explanations for these intriguing behaviors, which call for a deeper examination of tomography in a variety of strongly interacting quark-gluon systems.

Introduction.— Hadrons compose nearly all the visible matter in the universe, yet much is still unknown about them. Revealing their internal structure from experimental data requires the use of sophisticated theoretical frameworks based on quantum chromodynamics (QCD), the theory of the strong force of quarks and gluons (partons), that describe hadrons as emergent phenomena. While decades of high-energy experiments have provided data allowing for the high resolution of the longitudinal structure of protons [1–6], and to a lesser extent also of pions [7–18], the information on the transverse structure of hadrons is comparatively less well known. In particular, achieving a 3-dimensional mapping of internal hadron structure requires sensitivity to both collinear and transverse parton degrees of freedom, which can be encoded in transverse momentum dependent distributions (TMDs) [19–23] and generalized parton distributions (GPDs) [24, 25]. Both are primary focuses at existing and future facilities, such as Jefferson Lab [26] and the Electron-Ion Collider [27]. Here we focus on TMDs and novel properties of the transverse separation of quark fields as a function of their longitudinal momenta for the proton and pion, giving deeper insights into color confined systems that emerge from QCD.

TMDs depend on both the longitudinal momentum fraction x and the intrinsic transverse momentum $k_T \equiv |\boldsymbol{k}_T|$ of partons inside the hadron. The unpolarized TMD PDF is the k_T-space Fourier transform of the light-front correlator of hadron $\mathcal{N}$ (with momentum P) [21, 23],

$$\tilde{f}_{q/\mathcal{N}}(x, b_T) = \int \frac{\mathrm{d}b^-}{4\pi}\, e^{-ixP^+b^-}\, \mathrm{Tr}\big[\langle \mathcal{N}\,|\,\bar{\psi}_q(b)\gamma^+\mathcal{W}(b,0)\psi_q(0)\,|\,\mathcal{N}\rangle\big], \tag{1}$$

where $b \equiv (b^-, 0^+, \boldsymbol{b}_T)$, with $\boldsymbol{b}_T$ the transverse shift of the quark field ψ_q, and $b_T \equiv |\boldsymbol{b}_T|$. The Wilson line $\mathcal{W}(b,0)$ ensures SU(3) color gauge invariance. The TMDs in Eq. (1) require a modification to account for the ultraviolet and rapidity divergenes, and acquire corresponding regulators $\tilde{f}_{q/\mathcal{N}}(x, b_T) \to \tilde{f}_{q/\mathcal{N}}(x, b_T; \mu, \zeta)$ [23, 28].

While $\tilde{f}_{q/\mathcal{N}}$ is technically the object to be inferred from data, its small-b_T behavior can be written in terms of collinear PDFs [23, 29, 30]. Most phenomenological extractions to date [31–38] have made use of this connection by fixing the collinear PDFs and focusing on the analysis of the nonperturbative large-b_T region. However, these extractions are subject to the choices of the input collinear PDFs, as discussed in Ref. [39].

In this Letter, we go beyond the previous studies by performing the first simultaneous extraction of proton and pion TMD PDFs, along with pion collinear PDFs, through an analysis of fixed-target Drell-Yan (DY) and leading neutron (LN) data within the JAM QCD analysis framework [6, 14, 16–18, 40–57]. We find an intriguing behavior of the average transverse separation of the quark fields encoded in these TMD PDFs, with $\sim (5.3 - 7.5)\,\sigma$ smaller values for the pion than for the proton as a function of x. For both systems the average transverse separation of the quark field decreases as x decreases. We also observe a nuclear modification of the TMDs, with the average transverse separation of a quark field in a bound proton up to 10% smaller than that in a free proton.

Analysis framework.— The focus of our analysis is the DY process in hadron-hadron or hadron-nucleus reactions with center of mass energy $\sqrt{s}$. Specifically, we study the region of small transverse momentum q_T of the produced lepton pair relative to its invariant mass Q. In this regime, the measured cross section can be described in terms of TMDs through a well-defined factorization

framework [23, 58, 59]. Schematically, the DY cross section for hadron ($\mathcal{N} = \pi, p$)–nucleus (A) collisions differential in Q^2, rapidity of the lepton pair y, and q_T is given by

$$\frac{\mathrm{d}^3\sigma}{\mathrm{d}Q^2\mathrm{d}y\mathrm{d}q_T^2} = \sum_q \mathcal{H}_{q\bar{q}}(Q,\mu_Q)\int\frac{\mathrm{d}^2\boldsymbol{b}_T}{(2\pi)^2}\,e^{i\boldsymbol{b}_T\cdot\boldsymbol{q}_T} \times \tilde{f}_{q/\mathcal{N}}(x_{\mathcal{N}},b_T,\mu_Q,Q^2)\,\tilde{f}_{\bar{q}/A}(x_A,b_T,\mu_Q,Q^2)\,. \quad (2)$$

Here, the hard factor $\mathcal{H}_{q\bar{q}}$ represents the parton-level reaction that is factorized from the process-independent TMDs $\tilde{f}_{q(\bar{q})/\mathcal{N}(A)}$. The longitudinal momentum fractions of the TMDs are kinematically constrained to be $x_{\mathcal{N}(A)} = \sqrt{\tau}e^{+(-)y}$, where $\tau = Q^2/s$. Additionally, to optimize the perturbative calculation, the scale dependence is set as $\mu_Q = Q$ and the rapidity scale $\zeta = Q^2$ [23].

We use the standard $b_* = b_T/\sqrt{1+b_T^2/b_{\rm max}^2}$ prescriptionto model the large-b_T behavior of the TMDs, and following Ref. [60] we take

$$\tilde{f}_{q/\mathcal{N}(A)}(x,b_T,\mu_Q,Q^2) = (C\otimes f)_{q/\mathcal{N}(A)}(x;b_*) \times\exp\left\{-g_{q/\mathcal{N}(A)}(x,b_T)-g_K(b_T)\ln\frac{Q}{Q_0}-S(b_*,Q,\mu_Q)\right\}. \quad (3)$$

Here, the first line is the operator product expansion (OPE) [23, 29, 30], which describes the small-b_T behavior of the TMDs in terms of the collinear PDFs $f_{q/\mathcal{N}(A)}$ convoluted with perturbative Wilson coefficients C. The first two terms in the second line are nonperturbative functions to be extracted from experimental data: $g_{q/\mathcal{N}(A)}$ [23] that describes the deviation from the OPE at large b_T, and the nonperturbative part g_K of the Collins-Soper (CS) kernel [23]. The factor S contains the perturbative effects of soft gluon radiation, which can be written as

$$S(b_*,Q,\mu_Q) = -\tilde{K}(b_*;\mu_{b_*})\ln\frac{Q}{\mu_{b_*}} + \int_{\mu_{b_*}}^{\mu_Q}\frac{d\mu'}{\mu'}\left[-\gamma_f(\alpha_s(\mu');1)+\ln\frac{Q}{\mu'}\gamma_K(\alpha_s(\mu'))\right], \quad (4)$$

where $\mu_{b_*} = 2e^{-\gamma_E}/b_*$, the cusp anomalous dimension γ_K [61–66], the anomalous dimension of the TMD operator γ_f [23, 60, 67], and the perturbative part $\tilde{K}$ of the CS kernel [23, 60, 68, 69]. In our analysis we implement next-to-next-to-leading-logarithmic (N^{2}LL) accuracy for TMD PDFs by using γ_K at $\mathcal{O}(\alpha_s^3)$ and γ_f and $\tilde{K}$ at $\mathcal{O}(\alpha_s^2)$ precision. The hard factor $H_{q\bar{q}}$ in Eq. (2) is taken at $\mathcal{O}(\alpha_s)$ [23, 60]. The number of active flavors is determined by the hard scale Q. We use the starting scale $Q_0 = 1.27$ GeV and $b_{\rm max} = 2e^{-\gamma_E}/Q_0 \approx 0.88$ GeV^{-1}.

Since we use πA and pA DY data, we cannot extract TMDs for p,π,A systems simultaneously from two independent processes. We therefore relate the TMD PDFs for the nucleus to bound proton and neutron TMD PDFs (and use the isospin relations) by $\tilde{f}_{q/A} \equiv (Z/A)\tilde{f}_{q/p/A} + (1-Z/A)\tilde{f}_{q/n/A}$, for a nucleus with mass number A and atomic number Z. Our modeling for the nuclear dependence proceeds as follows: In the large-b_T region, we introduce a nuclear dependence on the quantity $g_{q/\mathcal{N}/A} = g_{q/\mathcal{N}}(1+a_{\mathcal{N}}(A^{1/3}-1))$, where $a_{\mathcal{N}}$ is a fit parameter [70]. The quantity g_K is universal regardless of the system, so we do not modify it. In the small-b_T region controlled by nuclear collinear PDFs, we describe the quarks in the bound nucleons inside the nuclei using the isospin relationship, e.g. $f_{u/p/A} = \frac{Z}{2Z-A}f_{u/A} + \frac{Z-A}{2Z-A}f_{d/A}$. Here, $f_{q/A}$ is taken from the EPPS16 analysis [71]. To be consistent with EPPS16, we utilize the CT14 at NLO [1] proton PDFs in the pA reactions. We consequently use the Wilson coefficeints in the OPE at $\mathcal{O}(\alpha_s)$.

In the collinear sector, our treatment for the q_T-integrated DY cross section includes threshold resummation in the double Mellin approach [17, 72]. For the LN reactions, we utilize the combined chiral effective theory and collinear factorization to describe the Sullivan process [73, 74].

We employ the Bayesian Monte Carlo (MC) methodology of the JAM Collaboration [6, 14, 16–18, 40–57]. To explore the model dependence of our extractions, we implement a variety of intrinsic nonperturbative functions: Gaussian [75–78], exponential, an interpolation of Gaussian-to-exponential [33, 37], Bessel-like [79–83], and a sum of Gaussians (MAP parametrization) [35]. In addition, we explore parametrizing g_K using a Gaussian [35, 76, 78], exponential [33, 37], and logarithm [79, 84, 85] at large-b_T. A detailed comparison of all the aforementioned parametrizations will be in a forthcoming paper.

Phenomenology.— As mentioned previously, we are including both q_T-dependent and collinear data, and are consequently able to for the first time to simultaneously extract the pion's TMD PDFs and collinear PDFs. In Tab. I we summarize all of the datasets that included in our analysis.

We use data from the E288 experiment [86] taken with 200, 300, and 400 GeV proton beams on a platinum (Pt) target, the E605 experiment [87] taken on a copper (Cu) target, and the E772 experiment [88] using a deuterium target expressed as $E\mathrm{d}^3\sigma/\mathrm{d}^3\mathbf{q} = (1/\pi)\mathrm{d}^2\sigma/\mathrm{d}y\mathrm{d}q_T^2$, which can be related to Eq. (2). The E288 and E605 experiments are measured with fixed rapidity and fixed $x_F = 2\sqrt{\tau}\sinh(y)$, respectively, while the E772 experiment measured over $0.1 \le x_F \le 0.3$.

This analysis also includes the ratios $R_{A,B} = (\mathrm{d}\sigma/\mathrm{d}q_T)|_{pA}/(\mathrm{d}\sigma/\mathrm{d}q_T)|_{pB}$ of DY cross section per nucleon from an 800 GeV proton beam incident on beryllium (Be), iron (Fe), and tungsten (W) targets from the E866 experiment [89]. These datasets are particularly sensitive to nuclear TMDs [70]. We integrate over the Q range for each bin and the measured $0 < x_F < 0.8$ range.

To constrain the pion TMDs, we include q_T-dependent DY data from the E615 [90] and E537 [91]. While these

experiments also measured $\mathrm{d}^2\sigma/\mathrm{d}Q\mathrm{d}q_T$, the observables we consider are $\mathrm{d}^2\sigma/\mathrm{d}x_F\mathrm{d}q_T$. In the Q-dependent cross section, an integration over $0 < x_F < 1$ would be required, the upper limit of which is not well defined in the factorization approach. On the other hand, the range of Q integration for the x_F-dependent cross section is well within a region where factorization is valid. Complementary to the q_T-differential data, we include the pion-induced q_T-integrated DY data from the E615 and NA10 [92] experiments measuring $\mathrm{d}^2\sigma/\mathrm{d}\sqrt{\tau}\mathrm{d}x_F$, which strongly constrain the pion's valence quark distributions. We also analyze the LN electroproduction data from HERA [93, 94] as in previous JAM analyses [14, 16–18].

To ensure the validity of TMD factorization, we impose a cut [37] on the data to small-q_T: $q_{T,\max} < 0.25\,Q$, where $q_{T,\max}$ is the upper bound of the q_T bin. We restrict our analysis to data in the range $4 < Q < 9$ GeV and $Q > 11$ GeV in order to avoid the region of J/ψ and Υ resonances. As was done in Ref. [37], we impose a cut on the q_T-dependent DY data of $x_F < 0.8$ to avoid regions where threshold resummation may be additionally needed. However, since we include threshold effects for collinear DY observables, we extend their kinematic range to $0 < x_F < 0.9$ and use the range $4.16 < Q < 7.68$ GeV. We also impose cuts on the LN data as was done in previous works [14, 16–18].

In summary, we analyze 383 q_T-dependent pion-induced and proton-nucleus DY data points, 117 q_T-integrated pion-induced DY data points, and 108 data points from the LN experiments, totalling 608 data points. In exploring the nonperturbative parmaetrizations mentioned above, we observed that the Gaussian g_K and multi-component (sum of Gaussians) MAP-like [35] flavor-independent parametrizations for the intrinsic $g_{q/\mathcal{N}}$ have the best agreement across all q_T-dependent observables. We do not find any significant improvement in the description of the data with the inclusion of flavor dependence. This corresponds to 11 parameters for $g_{q/\mathcal{N}}$ plus one parameter for nuclear dependence, one parameter for g_K to model the TMDs, along with an additional 8 parameters for pion collinear PDFs, and one LN cutoff parameter.

The resulting agreement with the data is shown in Tab. I where the χ^2 per number of points (N) and the Z-scores are provided for each of the experimental datasets considered in this work. The Z-score is the inverse of the normal cumulative distribution function, $Z = \Phi^{-1}(p) \equiv \sqrt{2}\ \mathrm{erf}^{-1}(2p-1)$, where the p-value is computed according to the resulting χ^2 shown in Tab. I. The Z-score describes the significance of the χ^2 relative to the expected χ^2 distribution. Our analysis shows a relatively good compatibility between data and theory at the level of Z-score of 2.6, with a total $\chi^2/N = 1.15$. The worst agreement to the datasets we found was to the E772 data, which provided a Z-score of above 5. Other analyses [33, 35] also showed a difficulty in obtaining agreement, which may be related to an experimental data issue.

TABLE I. Resulting χ^2 and Z-scores for the MC analysis.

Process	Experiment	$\sqrt{s}$ (GeV)	χ^2/N	Z-score
TMD				
q_T-*dep. pA DY*	E288 [86]	19.4	0.93	0.25
$pA \to \mu^+\mu^- X$	E288 [86]	23.8	1.33	1.54
	E288 [86]	24.7	0.95	0.23
	E605 [87]	38.8	1.07	0.39
	E772 [88]	38.8	2.41	5.74
(Fe/Be)	E866 [89]	38.8	1.07	0.29
(W/Be)	E866 [89]	38.8	0.89	0.11
q_T-*dep.* πA *DY*	E615 [90]	21.8	1.61	2.58
$\pi W \to \mu^+\mu^- X$	E537 [91]	15.3	1.11	0.57
Collinear				
q_T-*integr. DY*	E615 [90]	21.8	0.86	0.76
$\pi W \to \mu^+\mu^- X$	NA10 [92]	19.1	0.54	2.27
	NA10 [92]	23.2	0.91	0.18
Leading neutron	H1 [93]	318.7	0.36	4.61
$ep \to e'nX$	ZEUS [94]	300.3	1.48	2.16
Total			1.15	2.55

We find that there is no substantial impact on the collinear pion PDFs from the inclusion of the q_T-dependent data. This indicates that the TMD and collinear regimes are well separated in the data we analyzed, in contrast to the high-energy analysis [39], and that the measurements correlate more strongly with TMDs than collinear PDFs.

Results and discussion.— The definition of the TMD PDF is a 2-dimensional number density dependent on x and b_T. Under Bayes' theorem we can define a conditional density $\tilde{f}_{q/\mathcal{N}}(b_T|x)$ dependent on "b_T given x" as the following ratio:

$$\tilde{f}_{q/\mathcal{N}}(b_T|x;Q,Q^2) \equiv \frac{\tilde{f}_{q/\mathcal{N}}(x,b_T;Q,Q^2)}{\int \mathrm{d}^2\boldsymbol{b}_T \tilde{f}_{q/\mathcal{N}}(x,b_T;Q,Q^2)}\,. \tag{5}$$

Notice that this conditional probability is normalized such that $\int \mathrm{d}^2\boldsymbol{b}_T \tilde{f}_{q/\mathcal{N}}(b_T|x;Q,Q^2) = 1$.

We show in Fig. 1 the extracted proton and pion conditional densities for the up quark $\tilde{f}_{u/\mathcal{N}}(b_T|x;Q,Q^2)$ in the region covered by the experimental data $x \in [0.3, 0.6]$. Each TMD PDF is shown with its 1σ uncertainty band from the analysis. We focus here on the up quark since our analysis does not include flavor separation in the nonperturbative contribution to the TMDs. One can see that the pion TMD PDF is significantly narrower in b_T compared to the proton and both become wider with increasing values of x. To make quantitative comparisons between the distributions of the two hadrons, we show in Fig. 2 the conditional average b_T as a function of x, defined as

$$\langle b_T|x\rangle_{q/\mathcal{N}} = \int \mathrm{d}^2\boldsymbol{b}_T\, b_T\, \tilde{f}_{q/\mathcal{N}}(b_T|x;Q,Q^2) \tag{6}$$

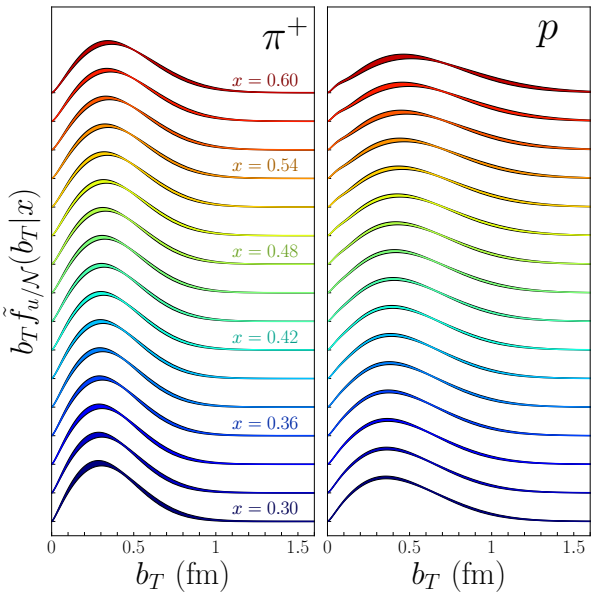

FIG. 1. The conditional TMD PDFs for the pion (**left**) and proton (**right**) as a function of b_T for various x values (indicated by color) evaluated at a characteristic experimental scale $Q = 6$ GeV. Each of the TMD PDFs are offset for visual purposes.

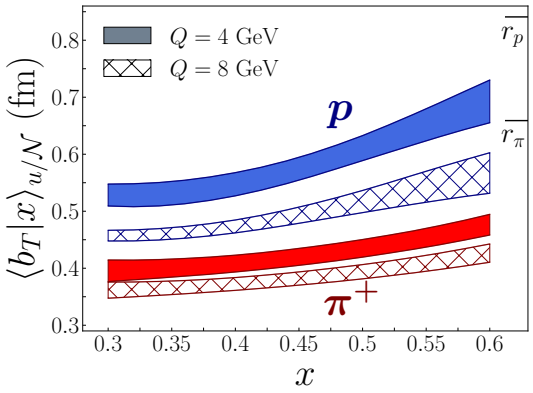

FIG. 2. The conditional average b_T calculated by Eq. (6) for the up quark in the proton (upper, blue) and in the pion (lower, red) for two Q values as a function of x. We also include r_p and r_π are the PDG values [95] of the charge radii for each hadron for reference.

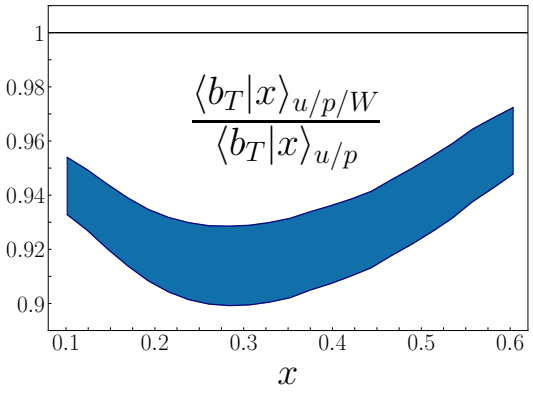

FIG. 3. The ratio of the conditional average b_T of the up quark in a proton bound in a tungsten nucleus to that of the free proton at $Q = 4$ GeV.

for the up quark. We find that in the proton the correlations among the up quarks in the transverse plane have a wider range compared to those in the pion. On average, there is a $\sim 20\%$ reduction of the up quark transverse correlations in pions relative to protons within a $\sim 5.3 - 7.5\ \sigma$ confidence level. We note that this value is approximately the same as the ratio of the charge radii of the pion and proton from the nominal values in the PDG ($r_p = 0.8409\ \pm\ 0.0004$ fm, $r_\pi = 0.659\ \pm\ 0.004$ fm) [95]. Also, within each hadron, the average spatial separation of quark fields in the transverse direction does not exceed its charge radius, as shown on the right edge of Fig. 2.

The growing behavior of the transverse correlations in the $x \to 1$ region is because the phase space for the transverse motion of partons becomes smaller since most of the momentum is along the light-cone direction. Furthermore, as Q increases, more gluons are radiated, which makes TMD PDFs wider in k_T space and therefore narrower in b_T space. Both of these features are quantitatively confirmed by our results in Fig. 2. It is important to note we checked that the differences between the proton and pion $\langle b_T|x\rangle$ are completely due to the nonperturbative TMD structure, independent of the collinear PDFs.

In Ref. [96] it was proposed that apart from the size of the nucleon, there exists an additional characteristic smaller scale in QCD associated with $q\bar{q}$ condensates. This suggests a possible explanation of the observed monotonically decreasing behavior of $\langle b_T|x\rangle$ with decreasing values of x, since, in this picture, once sea quarks emerge in the wave function, the quark q can only be shifted by a reduced transverse distance. However, more work is needed in order to firmly establish a connection between $q\bar{q}$ condensates and TMDs.

In Fig. 3 we analyze the effect the nuclear environment has on the transverse correlations of quarks inside nucleons, i.e., a possible transverse EMC effect, by taking the ratio of $\langle b_T|x\rangle$ for a bound proton in a nucleus to that of a free proton. We find an analogous suppression around $x \sim 0.3$, similar to that found in the collinear distributions [97]. We have verified that this effect is genuinely produced by the non-perturbative nuclear dependence in the TMD and not from the collinear dependence in the OPE. Our results are consistent with the findings in Ref. [70]. However, in this work, we went one step beyond their analysis by studying the x-dependence of the non-perturbative transverse structure within the

simultaneous collinear and TMD QCD global analysis framework.

Conclusions.— We have presented a comprehensive analysis of proton and pion TMD PDFs at N^{2}LL perturbative precision using fixed-target DY data. This analysis for the first time used both q_T-integrated and q_T-differential DY data, as well as LN measurements, to simultaneously extract pion collinear and TMD PDFs and proton TMD PDFs. The combined analysis, including an exploration of the nuclear dependence of TMDs, allowed us to perform a detailed comparison of proton and pion TMDs and to study the similarities and differences of their transverse momentum dependence.

In summary, we have determined conclusively that the transverse correlations of quarks in a pion are 20% smaller than those in a proton with a more than 5σ confidence level. The observed characteristic decrease of the average separation of quark fields for decreasing x may indicate the influence of the quark-antiquark condensate [96]. This calls for more scrutiny in the connection between our results and these theoretical expectations. We also found evidence for the transverse EMC effect as earlier pointed out by results in Ref. [70].

Here, we explored the quark transverse correlations restricted to two available hadronic systems. In the near future, when the tagged SIDIS program at Jefferson Lab and the EIC becomes available, we will be able to carry out similar analyses to include kaons, neutrons, and beyond. Such analyses, in combination with future lattice QCD calculations in the TMD sector, will provide a more complete picture of strongly interacting quark-gluon systems that emerge from QCD.

Acknowledgments.— We would like to acknowledge many useful discussions with Alexey Vladimirov, Zhongbo Kang, and Anatoly Radyushkin. This work has been supported by the U.S. Department of Energy under contracts No. DE-FG02-07ER41460 (LG, EM), No. DE-AC02-06CH11357 (EM), No. DE-AC05-06OR23177 (PB, WM, AP) under which Jefferson Science Associates, LLC, manages and operates Jefferson Lab, the National Science Foundation under Grants No. PHY-2011763 (DP) and No. PHY-2012002 (AP), and within the framework of the TMD Topical Collaboration. The work of NS was supported by the DOE, Office of Science, Office of Nuclear Physics in the Early Career Program.

[1] S. Dulat, T.-J. Hou, J. Gao, M. Guzzi, J. Huston, P. Nadolsky, J. Pumplin, C. Schmidt, D. Stump, and C. P. Yuan, Phys. Rev. D **93**, 033006 (2016), arXiv:1506.07443 [hep-ph].
[2] R. D. Ball *et al.*, Eur. Phys. J. C **77**, 663 (2017), arXiv:1706.00428 [hep-ph].
[3] S. Alekhin, J. Blümlein, S. Moch, and R. Placakyte, Phys. Rev. D **96**, 014011 (2017), arXiv:1701.05838 [hep-ph].
[4] T.-J. Hou *et al.*, Phys. Rev. D **103**, 014013 (2021), arXiv:1912.10053 [hep-ph].
[5] S. Bailey, T. Cridge, L. A. Harland-Lang, A. D. Martin, and R. S. Thorne, Eur. Phys. J. C **81**, 341 (2021), arXiv:2012.04684 [hep-ph].
[6] E. Moffat, W. Melnitchouk, T. C. Rogers, and N. Sato, Phys. Rev. D **104**, 016015 (2021), arXiv:2101.04664 [hep-ph].
[7] J. F. Owens, Phys. Rev. D **30**, 943 (1984).
[8] P. Aurenche, R. Baier, M. Fontannaz, M. N. Kienzle-Focacci, and M. Werlen, Phys. Lett. B **233**, 517 (1989).
[9] P. J. Sutton, A. D. Martin, R. G. Roberts, and W. J. Stirling, Phys. Rev. D **45**, 2349 (1992).
[10] M. Gluck, E. Reya, and A. Vogt, Z. Phys. C **53**, 651 (1992).
[11] M. Gluck, E. Reya, and I. Schienbein, Eur. Phys. J. C **10**, 313 (1999), arXiv:hep-ph/9903288.
[12] K. Wijesooriya, P. E. Reimer, and R. J. Holt, Phys. Rev. C **72**, 065203 (2005), arXiv:nucl-ex/0509012.
[13] M. Aicher, A. Schafer, and W. Vogelsang, Phys. Rev. Lett. **105**, 252003 (2010), arXiv:1009.2481 [hep-ph].
[14] P. C. Barry, N. Sato, W. Melnitchouk, and C.-R. Ji, Phys. Rev. Lett. **121**, 152001 (2018), arXiv:1804.01965 [hep-ph].
[15] I. Novikov *et al.*, Phys. Rev. D **102**, 014040 (2020), arXiv:2002.02902 [hep-ph].
[16] N. Y. Cao, P. C. Barry, N. Sato, and W. Melnitchouk, Phys. Rev. D **103**, 114014 (2021), arXiv:2103.02159 [hep-ph].
[17] P. C. Barry, C.-R. Ji, N. Sato, and W. Melnitchouk, Phys. Rev. Lett. **127**, 232001 (2021), arXiv:2108.05822 [hep-ph].
[18] P. C. Barry, C. Egerer, J. Karpie, W. Melnitchouk, C. Monahan, K. Orginos, J.-W. Qiu, D. G. Richards, N. Sato, R. S. Sufian and S. Zafeiropoulos, Phys. Rev. D **105**, 114051 (2022), arXiv:2204.00543 [hep-ph].
[19] A. Kotzinian, Nucl. Phys. B **441**, 234 (1995), arXiv:hep-ph/9412283.
[20] R. D. Tangerman and P. J. Mulders, Phys. Rev. D **51**, 3357 (1995), arXiv:hep-ph/9403227.
[21] P. J. Mulders and R. D. Tangerman, Nucl. Phys. B **461**, 197 (1996), [Erratum: Nucl.Phys.B 484, 538–540 (1997)], arXiv:hep-ph/9510301.
[22] D. Boer and P. J. Mulders, Phys. Rev. D **57**, 5780 (1998), arXiv:hep-ph/9711485.
[23] J. Collins, (2011), *Foundations of Perturbative QCD*, (Cambridge University Press, Cambridge, England, 2011).
[24] M. Diehl, Phys. Rept. **388**, 41 (2003), arXiv:hep-ph/0307382.
[25] A. V. Belitsky and A. V. Radyushkin, Phys. Rept. **418**, 1 (2005), arXiv:hep-ph/0504030.
[26] J. Dudek *et al.*, Eur. Phys. J. A **48**, 187 (2012), arXiv:1208.1244 [hep-ex].
[27] R. Abdul Khalek *et al.*, (2021), arXiv:2103.05419 [physics.ins-det].
[28] S. Aybat and T. C. Rogers, Phys.Rev. **D83**, 114042 (2011), arXiv:1101.5057 [hep-ph].
[29] J. C. Collins, D. E. Soper, and G. Sterman, Nucl. Phys. **B250**, 199 (1985).
[30] J. Collins and T. Rogers, Phys.Rev. **D91**, 074020 (2015), arXiv:1412.3820 [hep-ph].
[31] A. Bacchetta, F. Delcarro, C. Pisano, M. Radici, and

A. Signori, JHEP **06**, 081 (2017), [Erratum: JHEP 06, 051 (2019)], arXiv:1703.10157 [hep-ph].
[32] A. Bacchetta, V. Bertone, C. Bissolotti, G. Bozzi, F. Delcarro, F. Piacenza, and M. Radici, JHEP **07**, 117 (2020), arXiv:1912.07550 [hep-ph].
[33] V. Bertone, I. Scimemi, and A. Vladimirov, JHEP **06**, 028 (2019), arXiv:1902.08474 [hep-ph].
[34] I. Scimemi and A. Vladimirov, JHEP **06**, 137 (2020), arXiv:1912.06532 [hep-ph].
[35] A. Bacchetta, V. Bertone, C. Bissolotti, G. Bozzi, M. Cerutti, F. Piacenza, M. Radici, and A. Signori, (2022), arXiv:2206.07598 [hep-ph].
[36] X. Wang, Z. Lu, and I. Schmidt, JHEP **08**, 137 (2017), arXiv:1707.05207 [hep-ph].
[37] A. Vladimirov, JHEP **10**, 090 (2019), arXiv:1907.10356 [hep-ph].
[38] M. Cerutti, L. Rossi, S. Venturini, A. Bacchetta, V. Bertone, C. Bissolotti, and M. Radici, (2022), arXiv:2210.01733 [hep-ph].
[39] M. Bury, F. Hautmann, S. Leal-Gomez, I. Scimemi, A. Vladimirov, and P. Zurita, JHEP **10**, 118 (2022), arXiv:2201.07114 [hep-ph].
[40] P. Jimenez-Delgado, W. Melnitchouk, and J. F. Owens, J. Phys. G **40**, 093102 (2013), arXiv:1306.6515 [hep-ph].
[41] P. Jimenez-Delgado, A. Accardi, and W. Melnitchouk, Phys. Rev. D **89**, 034025 (2014), arXiv:1310.3734 [hep-ph].
[42] P. Jimenez-Delgado, H. Avakian, and W. Melnitchouk (Jefferson Lab Angular Momentum (JAM)), Phys. Lett. B **738**, 263 (2014), arXiv:1403.3355 [hep-ph].
[43] N. Sato, W. Melnitchouk, S. E. Kuhn, J. J. Ethier, and A. Accardi (Jefferson Lab Angular Momentum), Phys. Rev. D **93**, 074005 (2016), arXiv:1601.07782 [hep-ph].
[44] N. Sato, J. J. Ethier, W. Melnitchouk, M. Hirai, S. Kumano, and A. Accardi, Phys. Rev. D **94**, 114004 (2016), arXiv:1609.00899 [hep-ph].
[45] J. J. Ethier, N. Sato, and W. Melnitchouk, Phys. Rev. Lett. **119**, 132001 (2017), arXiv:1705.05889 [hep-ph].
[46] H.-W. Lin, W. Melnitchouk, A. Prokudin, N. Sato, and H. Shows, Phys. Rev. Lett. **120**, 152502 (2018), arXiv:1710.09858 [hep-ph].
[47] N. Sato, C. Andres, J. J. Ethier, and W. Melnitchouk (JAM), Phys. Rev. D **101**, 074020 (2020), arXiv:1905.03788 [hep-ph].
[48] J. Cammarota, L. Gamberg, Z.-B. Kang, J. A. Miller, D. Pitonyak, A. Prokudin, T. C. Rogers, and N. Sato, Phys. Rev. D **102**, 054002 (2020), arXiv:2002.08384 [hep-ph].
[49] J. Bringewatt, N. Sato, W. Melnitchouk, J.-W. Qiu, F. Steffens, and M. Constantinou, Phys. Rev. D **103**, 016003 (2021), arXiv:2010.00548 [hep-ph].
[50] D. Adamiak, Y. V. Kovchegov, W. Melnitchouk, D. Pitonyak, N. Sato, and M. D. Sievert (Jefferson Lab Angular Momentum), Phys. Rev. D **104**, L031501 (2021), arXiv:2102.06159 [hep-ph].
[51] C. Cocuzza, C. E. Keppel, H. Liu, W. Melnitchouk, A. Metz, N. Sato, and A. W. Thomas, Phys. Rev. Lett. **127**, 242001 (2021), arXiv:2104.06946 [hep-ph].
[52] Y. Zhou, C. Cocuzza, F. Delcarro, W. Melnitchouk, A. Metz, and N. Sato (Jefferson Lab Angular Momentum (JAM)), Phys. Rev. D **104**, 034028 (2021), arXiv:2105.04434 [hep-ph].
[53] C. Cocuzza, W. Melnitchouk, A. Metz, and N. Sato (Jefferson Lab Angular Momentum (JAM)), Phys. Rev. D **104**, 074031 (2021), arXiv:2109.00677 [hep-ph].
[54] Y. Zhou, N. Sato, and W. Melnitchouk (Jefferson Lab Angular Momentum (JAM)), Phys. Rev. D **105**, 074022 (2022), arXiv:2201.02075 [hep-ph].
[55] M. Boglione, M. Diefenthaler, S. Dolan, L. Gamberg, W. Melnitchouk, D. Pitonyak, A. Prokudin, N. Sato, and Z. Scalyer (Jefferson Lab Angular Momentum (JAM)), JHEP **04**, 084 (2022), arXiv:2201.12197 [hep-ph].
[56] C. Cocuzza, W. Melnitchouk, A. Metz, and N. Sato (Jefferson Lab Angular Momentum (JAM)), Phys. Rev. D **106**, L031502 (2022), arXiv:2202.03372 [hep-ph].
[57] L. Gamberg, M. Malda, J. A. Miller, D. Pitonyak, A. Prokudin, and N. Sato, Phys. Rev. D **106**, 034014 (2022), arXiv:2205.00999 [hep-ph].
[58] X.-d. Ji, J.-P. Ma, and F. Yuan, Phys. Lett. B **597**, 299 (2004), arXiv:hep-ph/0405085.
[59] M. G. Echevarria, A. Idilbi, and I. Scimemi, JHEP **07**, 002 (2012), arXiv:1111.4996 [hep-ph].
[60] J. Collins and T. C. Rogers, Phys. Rev. D **96**, 054011 (2017), arXiv:1705.07167 [hep-ph].
[61] A. M. Polyakov, Nucl. Phys. B **164**, 171 (1980).
[62] G. P. Korchemsky and A. V. Radyushkin, Phys. Lett. B **171**, 459 (1986).
[63] G. P. Korchemsky and A. V. Radyushkin, Nucl. Phys. B **283**, 342 (1987).
[64] J. C. Collins, Adv. Ser. Direct. High Energy Phys. **5**, 573 (1989), arXiv:hep-ph/0312336.
[65] S. Moch, J. A. M. Vermaseren, and A. Vogt, Nucl. Phys. B **688**, 101 (2004), arXiv:hep-ph/0403192.
[66] J. M. Henn, G. P. Korchemsky, and B. Mistlberger, JHEP **04**, 018 (2020), arXiv:1911.10174 [hep-th].
[67] S. Moch, J. A. M. Vermaseren, and A. Vogt, JHEP **08**, 049 (2005), arXiv:hep-ph/0507039.
[68] J. C. Collins and D. E. Soper, Nucl. Phys. **B193**, 381 (1981).
[69] J. C. Collins and D. E. Soper, Nucl. Phys. **B194**, 445 (1982).
[70] M. Alrashed, D. Anderle, Z.-B. Kang, J. Terry, and H. Xing, Phys. Rev. Lett. **129**, 242001 (2022).
[71] K. J. Eskola, P. Paakkinen, H. Paukkunen, and C. A. Salgado, Eur. Phys. J. C **77**, 163 (2017), arXiv:1612.05741 [hep-ph].
[72] D. Westmark and J. F. Owens, Phys. Rev. D **95**, 056024 (2017), arXiv:1701.06716 [hep-ph].
[73] J. D. Sullivan, Phys. Rev. D **5**, 1732 (1972).
[74] J. R. McKenney, N. Sato, W. Melnitchouk, and C.-R. Ji, Phys. Rev. D **93**, 054011 (2016), arXiv:1512.04459 [hep-ph].
[75] C. T. H. Davies, B. R. Webber, and W. J. Stirling, Nucl. Phys. B **256**, 413 (1985).
[76] P. M. Nadolsky, D. Stump, and C. Yuan, Phys.Rev. **D61**, 014003 (2000), arXiv:hep-ph/9906280 [hep-ph].
[77] F. Landry, R. Brock, P. M. Nadolsky, and C. P. Yuan, Phys. Rev. **D67**, 073016 (2003), arXiv:hep-ph/0212159.
[78] M. Anselmino, M. Boglione, J. Gonzalez H., S. Melis, and A. Prokudin, JHEP **1404**, 005 (2014), arXiv:1312.6261 [hep-ph].
[79] C. A. Aidala, B. Field, L. P. Gamberg, and T. C. Rogers, Phys. Rev. D **89**, 094002 (2014), arXiv:1401.2654 [hep-ph].
[80] P. Sun, J. Isaacson, C. P. Yuan, and F. Yuan, Int. J. Mod. Phys. A **33**, 1841006 (2018), arXiv:1406.3073 [hep-ph].
[81] A. V. Radyushkin, Phys. Lett. B **735**, 417 (2014),

arXiv:1404.7032 [hep-ph].
[82] A. Radyushkin, Phys. Lett. B **767**, 314 (2017), arXiv:1612.05170 [hep-ph].
[83] M. Boglione, J. O. Gonzalez-Hernandez, and A. Simonelli, Phys. Rev. D **106**, 074024 (2022), arXiv:2206.08876 [hep-ph].
[84] Z.-B. Kang, A. Prokudin, P. Sun, and F. Yuan, Phys. Rev. D **91**, 071501 (2015), arXiv:1410.4877 [hep-ph].
[85] Z.-B. Kang, A. Prokudin, P. Sun, and F. Yuan, Phys. Rev. D **93**, 014009 (2016), arXiv:1505.05589 [hep-ph].
[86] A. S. Ito *et al.*, Phys. Rev. D **23**, 604 (1981).
[87] G. Moreno *et al.*, Phys. Rev. D **43**, 2815 (1991).
[88] P. L. McGaughey *et al.*, Phys. Rev. D **50**, 3038 (1994), [Erratum: Phys.Rev.D 60, 119903 (1999)].
[89] M. A. Vasilev *et al.*, Phys. Rev. Lett. **83**, 2304 (1999), arXiv:hep-ex/9906010.
[90] J. S. Conway *et al.*, Phys. Rev. D **39**, 92 (1989).
[91] E. Anassontzis *et al.*, Phys. Rev. D **38**, 1377 (1988).
[92] B. Betev *et al.*, Z. Phys. C **28**, 9 (1985).
[93] F. D. Aaron *et al.*, Eur. Phys. J. C **68**, 381 (2010), arXiv:1001.0532 [hep-ex].
[94] S. Chekanov *et al.*, Nucl. Phys. **B637**, 3 (2002), arXiv:hep-ex/0205076.
[95] R. L. Workman *et al.* (Particle Data Group), PTEP **2022**, 083C01 (2022).
[96] P. Schweitzer, M. Strikman, and C. Weiss, JHEP **01**, 163 (2013), arXiv:1210.1267 [hep-ph].
[97] J. J. Aubert *et al.*, Phys. Lett. B **123**, 275 (1983).